ELEKTROTEHNIŠKI VESTNIK 89(5): 225-232, 2022
ORIGINAL SCIENTIFIC PAPER

Two Robust Methods to Control and Observe the Magnetic Flux and Rotational Speed of the Induction Motor Using a Four-Parameter Model

Ymene Kebbati[1], Yamna Hammou[2]

[1] *Automatic Department, University of Sciences and Technology of Oran (USTO-MB), Algeria.*
[2] *Maritime Engineering Department, University of Sciences and Technology of Oran (USTO-MB), Algeria.*
E-mail: ymenne.kebbati@univ-usto.dz

Abstract: The paper presents two methods to observe the magnetic flux and rotational speed of the induction motor using an inverse T-model. A direct vector control and the sliding-mode control are used. The observer is of an exponential order. Its gain is determined the nominal and high-speed operation. The low-speed operation is stabilized. The effectiveness of the control and observation algorithm is successfully verified by simulations and comparison with experimental results.

Keywords: induction motor, four parameters, field-oriented control, sliding mode control, high gain observer.

Metodi za nadzor in opazovanje magnetnega pretoka in vrtilne hitrosti indukcijskega motorja z uporabo modela s štirimi parametri

V prispevku predstavljamo dve metodi opazovanja magnetnega pretoka in vrtilne hitrosti indukcijskega motorja z inverznim T-modelom. Metodi temeljita na neposrednem vektorskem krmiljenju in krmiljenju v drsnem načinu. Izkoristek smo določili pri nominalni in visoki hitrosti delovanja. Delovanje pri nizki hitrosti je stabilizirano. Učinkovitost algoritma smo preverili v postopku simulacije in z eksperimentalnimi meritvami..

1 INTRODUCTION

For the control of the asynchronous machine to be efficient a high-order nonlinear model should be used and relation coupling between the different magnitudes known. The machine parameters generally depend on the operating point and vary as a function of the temperature machine (resistance) and magnetic state (inductance), and load variability can be variable. These variations negatively affect the performance of system r when using an invariable-parameter controller. New industrial applications require position/speed variations of a high-performance dynamics, good steady-state precision, high overload capacity, and robustness to various disturbances. Thus, why robust control algorithms is desirable both in stabilization and in trajectory following [1]. Most induction motor control schemes require accurate information the motor state variables and parameters. Fluxes are usually estimated based on measured stator currents and voltages [2-3], [5-6]. However, as they considerably depend on the motor model, parameter variations inevitably involve flux estimation. A rotor and stator resistance varies mainly as a function of the temperature. Thus, the idea of combining the theory of a four-parameter model, sliding mode technique and flux-oriented control provides a good possibility for a robust control for an induction motor of variable parameters [2].

In [8], a simple P-type dc-link overvoltage controller is proposed for a four-parameter model of the induction motor.

In [4], the speed-adaptive flux of the sensorless induction motor drive using a four-parameter model is estimated.

In [17], a reduced-order observer is used to estimate the rotor flux of the induction motor. It is shown that the flux dynamics form a nonlinear closed-loop system when estimating the flux field orientation. In [26, 27], use a high gain observer for a nonlinear system. [19] proposes mathematical models and algorithms to calculate processes and characteristics of the induction motor in a series compensation of the reactive power.

This paper presents a direct vector [3, 4] and a sliding-mode control both adapted to the four-parameter model to control the speed of the induction motor. In [10-12], a rotor flux observer for the induction motor is adapted to our four-parameter model and an experimental evaluation of the direct-vector and sliding mode control is presented. The results demonstrate the effectiveness of the proposed control model in terms of the system stability and robustness against parameter variations.

Received 27 June 2022
Accepted 7 November 2022

2 MATHEMATICAL Γ INVERSE MODEL OF INDUCTION MOTOR

For the squirrel cage-rotor motor, only four electrical parameters can be determined, which leaves a degree of freedom in determining the set of parameters [3]. The state matrix of the induction motor is of the dimension four and has four eigenvalues, there is an infinity of solutions with five parameters giving the same eigenvalues. To overcome this uncertainty, we use a four-parameter model [22] for minimize the leakage inductance towards [4] by reducing the coupling flux and rotor current. [4]- [14] - [15] - by:

$$\int_0^{r_2} F(r,\phi)\,\partial r\,\partial\phi = [\sigma r_2/(2\mu_0)]$$

$$\begin{cases} \varphi_R = k_r \varphi_r \\ i_R = \dfrac{i_r}{k_r} \end{cases} , with\ k_r = \frac{L_M}{L_r}$$

ϕ_R is the reduced rotor flux.

i_R is the reduced rotor current, k_r is the rotor magnetic coupling factor, L_M is the reduced magnetizing inductance, $L_M = k_r l_r$ and $R_R = k_r^2 R_r$ is its reduced rotor resistance, $L_S^{'}$ is the stator transient inductance:

$$L_S^{'} = \frac{k_r}{k}\ ,\ L_S = L_m + L_{s\sigma}\ ,\quad L_r = L_m + L_{r\sigma}$$

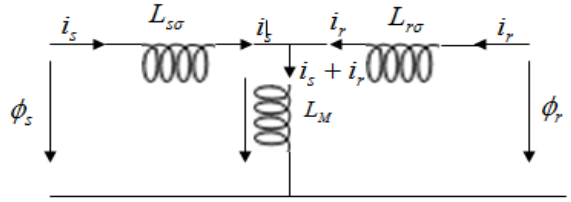

Figure 1. Flux linkage models, ***Γ*** model.

$L_{s\sigma}$ is the stator-leakage inductance and $L_{r\sigma}$ is the rotor leakage inductance. The four parameters become R_R , R_s $L_s^{'}$ and L_M .

And we have: $\tau_\sigma = \dfrac{L_S^{'}}{R_s + R_R}$ and $\tau_r = \dfrac{L_M}{R_R}$.

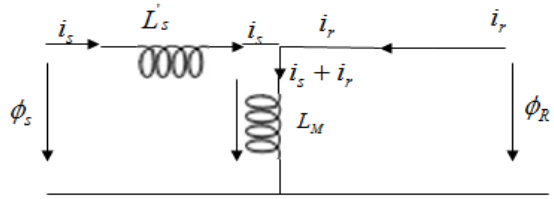

Figure 2. Flux-linkage models, inverse-***Γ*** model.

Thus, the final four parameters model in a rotating field (d, q) is defined by the equations in the state space:

$$\begin{bmatrix} \frac{\partial i_{sd}}{dt} \\ \frac{\partial i_{rd}}{dt} \\ \frac{\partial \varphi_{sd}}{dt} \\ \frac{\partial \varphi_{rd}}{dt} \end{bmatrix} = \begin{bmatrix} -\frac{1}{\tau_\sigma} & \omega_s & \frac{1}{L_s^{'}\tau_r} & \frac{P\Omega}{L_s^{'}} \\ \omega_s & -\frac{1}{\tau_\sigma} & -\frac{P\Omega}{L_s^{'}} & \frac{1}{L_s^{'}\tau_r} \\ R_R & 0 & -\frac{1}{\tau_\sigma} & (\omega_s + P\Omega) \\ 0 & R_R & -(\omega_s - P\Omega) & -\frac{1}{\tau_\sigma} \end{bmatrix} \begin{bmatrix} i_{sd} \\ i_{rd} \\ \varphi_{sd} \\ \varphi_{rd} \end{bmatrix} + \begin{bmatrix} \frac{1}{L_s^{'}} & 0 \\ 0 & \frac{1}{L_s^{'}} \\ 0 & 0 \\ 0 & 0 \end{bmatrix} \begin{bmatrix} U_{sd} \\ U_{sq} \end{bmatrix} \quad (1)$$

$$\frac{d\Omega}{dt} = \frac{p}{J_m}\varphi_{Rd} - \frac{f_m}{J_m}\Omega - \frac{T_L}{J_m}$$

2.1 State model in a fixed stator repository

In the frame of reference (α, β) fixed to the stator, the asynchronous motor model defined by the nonlinear system with four-parameter is:

$$\begin{bmatrix} \frac{\partial i_{s\alpha}}{dt} \\ \frac{\partial i_{r\beta}}{dt} \\ \frac{\partial \varphi_{s\alpha}}{dt} \\ \frac{\partial \varphi_{r\beta}}{dt} \end{bmatrix} = \begin{bmatrix} -\frac{1}{\tau_\sigma} & \omega_s & \frac{1}{L_s^{'}\tau_r} & \frac{P\Omega}{L_s^{'}} \\ \omega_s & -\frac{1}{\tau_\sigma} & -\frac{P\Omega}{L_s^{'}} & \frac{1}{L_s^{'}\tau_r} \\ R_R & 0 & -\frac{1}{\tau_\sigma} & -P\Omega \\ 0 & R_R & P\Omega & -\frac{1}{\tau_\sigma} \end{bmatrix} \begin{bmatrix} i_{s\alpha} \\ i_{r\beta} \\ \varphi_{s\alpha} \\ \varphi_{r\beta} \end{bmatrix} + \begin{bmatrix} \frac{1}{L_s^{'}} & 0 \\ 0 & \frac{1}{L_s^{'}} \\ 0 & 0 \\ 0 & 0 \end{bmatrix} \begin{bmatrix} U_{s\alpha} \\ U_{s\beta} \end{bmatrix} \quad (2)$$

3 PRINCIPLES OF THE VECTOR CONTROL ADAPTED TO THE FOUR-PARAMETER MODEL

For the vector control, a model of the induction motor is used in the coordinate system (d, q). It is obtained by using a reference frame connected to the rotating field whose axis d is aligned with the rotor flux vector:

$$\varphi_{Rq} = 0 \text{ and } \frac{\partial \varphi_{Rq}}{dt} = 0$$

$$\frac{\partial i_{sd}}{dt} = \frac{1}{\tau_\sigma} i_{sd} + \omega_s i_{sq} + \frac{1}{L_s^{'}\tau_r}\varphi_{rd} + \frac{P\Omega}{L_s^{'}} U_{sd} \quad (3)$$

$$\frac{\partial i_{sq}}{dt} = -\frac{1}{\tau_\sigma} i_{sq} - \omega_s i_{sd} - \frac{P\Omega}{L_s^{'}}\varphi_{rd} + \frac{1}{L_s^{'}} U_{sq} \quad (4)$$

$$\frac{\varphi_{Rd}}{dt} = R_R i_{sd} - \frac{1}{\tau_r}\varphi_{Rd} \quad (5)$$

$$0 = R_R i_{sq} - (\omega_s - P\Omega)\varphi_{Rd} \quad (6)$$

From Equation 6, we get :

$$\omega_s = P\Omega + \frac{R_R i_{sq}}{\varphi_{Rd}} \quad (7)$$

Therefore, the decoupled system becomes:

$$\begin{cases} \dfrac{di_{Sd}}{dt} = -\dfrac{1}{\tau_\sigma} i_{Sd} + v_d \\ \dfrac{d\varphi_{Rd}}{dt} = R_R i_{Sd} - \dfrac{1}{\tau_\sigma} \varphi_{Rd} \end{cases} \quad (8)$$

$$\begin{cases} \dfrac{di_{Sq}}{dt} = -\dfrac{1}{\tau_\sigma} i_{Sq} + v_q \\ \dfrac{d\Omega}{dt} = \dfrac{p}{J_{M\Omega}} \varphi_{Rd} i_{Sq} - \dfrac{f_m}{J_M} - \dfrac{T}{J_M} \end{cases} \quad (9)$$

With:

$$\begin{cases} v_d = \dfrac{1}{L_s'} \left[\dfrac{1}{L_s' \tau_r} \phi_{Rd} + p\Omega i_{sq} + \dfrac{R_R i_{sq}^2}{\phi_{Rd}} + u_{sd} \right] \\ v_q = \dfrac{1}{L_s'} \left[-\dfrac{p\Omega}{L_s'} \phi_{Rd} - p\Omega i_{sd} - \dfrac{R_R i_{sq} i_{sd}}{\phi_{Rd}} + u_{sq} \right] \end{cases} \quad (10)$$

Depending on how the position rotor flux is evaluated, there are two variants of the vector control. In the case of a direct control (FOC), the angle $\dot{\theta} = \omega_s$ is measured or estimated. In the case of an indirect control (IFOC), the angle is calculated from the expression of the slip speed (7) where $\dot{\theta} = \omega_s$. By replacing Equation 10 with Equation 7, we get the Usd and Usq commands:

$$\begin{pmatrix} u_{sd} \\ u_{sq} \end{pmatrix} = L_s' \begin{pmatrix} v_d - \dfrac{R_R i_{sq}^2}{\varphi_{Rd}} - \dfrac{1}{L_s' \tau_r} \varphi_{Rd} - p\Omega i_{sq} \\ v_q + \dfrac{R_R i_{sq} i_{sd}}{\varphi_{Rd}} + \dfrac{p\Omega}{L_s'} \varphi_{Rd} + p\Omega i_{sq} \end{pmatrix} \quad (11)$$

Using Equation 8 and 9, the rotor flux and speed are now controlled from the magnitudes of stator currents $H_1(s)$ respectively. The controls are performed by PI controllers shown in Figs. 3 and 4 respectively. The rotor flux control is ensured by two controllers, PI H_1 and H_3, such that:

$$\begin{cases} \hat{i}_{sd} = H_1(s) \left[\phi_{Rref} - \phi_{Rd} \right] \\ v_q = H_3(s) \left[\hat{i}_{sd} - i_{sd} \right] \end{cases} \quad (12)$$

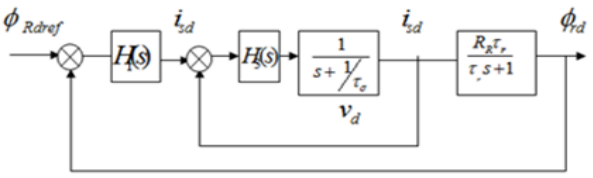

Figure 3. Flux control of the four-parameter model.

Where $\hat{i}_{sd}$ and ϕ_{ref} are the stator current and the reference flux in axis d, respectively.

The speed is controlled by two controllers Pi H_2 and H_4, such that:

$$\begin{cases} \hat{i}_{sq} = H_2(s)(\Omega_{ref} - \Omega) \\ v_q = H_4(s)(\hat{i}_{sq} - i_{sq}) \end{cases} \quad (13)$$

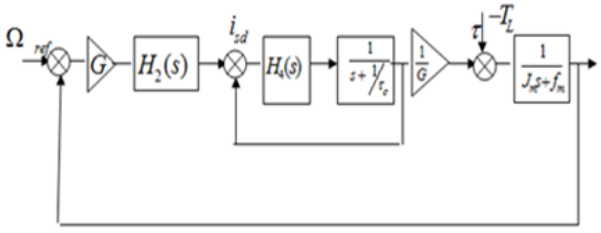

Figure 4. Speed control of the four-parameter model.

Where $\hat{i}_{sq}$ and Ω_{ref} are the stator current in axis q and the rotor reference speed.

Using the mechanical equation, the desired electromechanical torque is:

$$\tau_d = \frac{pM}{L_r} \phi_{ref} \hat{i}_{sq}$$

We obtain:

$$\tau_d = \frac{\hat{i}_{sq}}{G} \Rightarrow G = \frac{i_{sq}}{\tau_d}$$

4 Sliding-Mode Control Law Adapted to the Four-Parameter Model of the Induction Motor

An induction-motor model is used. It has four parameters in the reference (α, β) given by Equation 1, a control law based on the sliding-mode theory is:

$x = \begin{bmatrix} i_{s\alpha} & i_{s\beta} & \phi_{r\alpha} & \phi_{r\beta} & \Omega \end{bmatrix}^T$ is the state of the system.

$y = \begin{bmatrix} \Omega & \phi \end{bmatrix}^T$ is the output vector with $\varphi^2 = \phi_{r\alpha}^2 + \phi_{r\beta}^2$

It is assumed that all states of the system are measured. Our goal is to build control law $u = [u_a \quad u_h]^T$ to get the motor states, i.e. speed Ω and the norm of the rotor flux squared ϕ to join sliding surface $S = [S_1 \quad S_2]^T$

The states considered for the induction-motor control are the speed and the flux modulus.

4.1 Choice of the sliding surface

The sliding surface defined in [4] is;

$$S(x,t) = (\frac{\partial}{\partial t} + \lambda)e \tag{14}$$

where $\lambda = [\lambda_1 \quad \lambda_2]$ is a positive constant and

$$S = \frac{\partial y}{\partial t} - \frac{\partial y_d}{\partial t} + \lambda(y - y_d) \tag{15}$$

Then:

$$\begin{bmatrix} S_1 \\ S_2 \end{bmatrix} = \begin{bmatrix} \dot{\Omega} \\ \dot{\varphi} \end{bmatrix} - \begin{bmatrix} \dot{\Omega}_{ref} \\ \dot{\varphi}_{ref} \end{bmatrix} + \lambda \begin{bmatrix} \Omega - \Omega_{ref} \\ \varphi - \varphi_{ref} \end{bmatrix} \tag{16}$$

So:

$$\dot{\phi} = 2\varphi_{r\alpha}\dot{\varphi}_{r\alpha} + 2\varphi_{r\beta}\dot{\varphi}_{r\beta}$$

Substituting variables $\dot{\Omega}$ and $\dot{\phi}$ from system (1) in Equation 4, we have:

The sliding surfaces are given by:

$$\begin{cases} S_1 = x_1 - \frac{\tau_L}{p} - \frac{1}{\mu}\dot{\Omega}_{ref} + \frac{\lambda_1}{\mu}\left(\Omega - \Omega_{ref}\right) \\ S_2 = x_2 - \frac{1}{R_R\tau_r}\varphi - \frac{1}{2R_R}\dot{\varphi}_{ref} + \frac{\lambda_2}{2R_R}\left(\varphi - \varphi_{ref}\right) \end{cases} \tag{17}$$

With:

$x_1 = \varphi_{R_\alpha} i_{s\beta} - \varphi_{R\beta} i_{s\alpha}$, $x_2 = \varphi_{R_\alpha} i_{s\alpha} - \varphi_{R\beta} i_{s\beta}$, $\mu = \frac{p}{J_m}$,

$\phi = \varphi_{R\alpha}^2 + \varphi_{R\beta}^2$

The command is given by:

$$\begin{cases} u = u_{eq} + u_n \\ u_{eq} = -D^{-1}F \\ u_n = -D^{-1}\begin{bmatrix} u_{01} & 0 \\ 0 & u_{02} \end{bmatrix}\begin{bmatrix} sign(S_1) \\ sign(S_2) \end{bmatrix} \end{cases} \tag{18}$$

After calculating the derivate of $\dot{S}_1$ and $\dot{S}_2$, we get:

$$\begin{bmatrix} \dot{s}_1 \\ \dot{s}_2 \end{bmatrix} = \begin{bmatrix} A \\ B \end{bmatrix} + \frac{1}{L_s'}\begin{bmatrix} -\phi_{R\beta} & \phi_{R\alpha} \\ \phi_{R\alpha} & \phi_{R\beta} \end{bmatrix}\begin{bmatrix} u_{s\alpha} \\ u_{s\alpha} \end{bmatrix} \tag{19}$$

With:

$$\begin{cases} A = (\lambda_1 - \frac{1}{\tau_r} + \frac{1}{\tau_\sigma})x_1 - p\Omega(x_2 + \frac{1}{L_s'}\varphi) - \frac{\lambda_1\dot{\Omega}_{ref}}{\mu} - \frac{\ddot{\Omega}_{ref}}{\mu} - \frac{\lambda_1\tau_L}{\mu J_m} \\ B = (\lambda_2 - \frac{3}{\tau_r} + \frac{1}{\tau_\sigma})x_2 - p\Omega x_1 + R_R x_2 + (\frac{2}{\tau_r L_M} + \frac{1}{L_s'\tau_r} - \frac{\lambda_2}{L_M})\varphi - \frac{\lambda_2\varphi_{ref}}{2R_R} - \frac{\ddot{\varphi}_{ref}}{2R_R} \end{cases} \tag{20}$$

We have:

$$\dot{V}_C = (A - u_{01}sign(S_3))S_3 + (B - u_{02}sign(S_4))S_4 \tag{21}$$

For the values of u_{01} and u_{02} it is:

$$\begin{cases} u_{01} \succ |A| \\ u_{02} \succ |B| \end{cases}$$

By introducing the positive values, we get:

$$\begin{cases} \eta_1 = -(A - u_{01}sign(S_3)) \\ \eta_2 = -(B - u_{02}sign(S_4)) \end{cases} \tag{22}$$

By norming, expression Equation 19 becomes:

$$\dot{V} \le -\eta_1 |S_3| - -\eta_2 |S_4| \tag{23}$$

And:

$$V_1 = \frac{1}{2}S_3^2 \text{ and } V_2 = \frac{1}{2}S_4^2$$

So:

$$\dot{V}_c \le -\sqrt{2\eta_1}\sqrt{V_1} - -\sqrt{2\eta_2}\sqrt{V_2} \tag{24}$$

With $\eta = \max(\sqrt{2\eta_1}, \sqrt{2\eta_2})$, Equation 24 is written as:

$$\dot{V}_c \le -\eta(\sqrt{V_1} + \sqrt{V_2})$$

And : $(C\hat{Z} - y) = \begin{bmatrix} i_{s\alpha} - \hat{i}_{s\alpha} \\ i_{s\beta} - \hat{i}_{s\beta} \end{bmatrix}$

$\sqrt{V_1}+\sqrt{V_2} \le V_1+V_2$ when $V_i \ge 1$ such as $i=1,2$.

With $\dot{V}_c \le \eta V$.

Convergence η at a sliding surface is attractive.

4.2 Observer control with a high gain adapted to the four-parameter method

Synthesis of the observer control:

$$\begin{cases} \dot{Z} = F(\Omega)Z + G(u,\Omega,Z) \\ y = Cz \end{cases}$$

$$Z_1 = \begin{bmatrix} i_{s\alpha} & i_{s\beta} \end{bmatrix}^T ; Z_2 = \begin{bmatrix} \phi_{s\alpha} & \phi_{s\beta} \end{bmatrix}^T ;$$

$$U = \begin{bmatrix} u_{s\alpha} & u_{s\beta} \end{bmatrix}^T ; Y = \begin{bmatrix} i_{s\alpha} & i_{s\beta} \end{bmatrix}^T ; S = \Omega$$

The dynamics of the observer is:

$$\hat{Z} = F(\Omega)\hat{Z} + G(u,\Omega,\hat{Z}) - \Lambda^{-1} S_0^{-1} C^T (C\hat{Z} - Y)$$

With:

$$\Lambda = \begin{bmatrix} I_2 & 0 \\ 0 & F_1(\Omega) \end{bmatrix} ; S_0^{-1} C^T = \begin{bmatrix} 2\theta I_2 \\ \theta^2 I_2 \end{bmatrix}$$

And:

$$\Lambda(\Omega) = \begin{bmatrix} 0 & 0 & 0 & 0 \\ 0 & 1 & 0 & 0 \\ 0 & 0 & \frac{1}{L_s' \tau_r} & \frac{p\Omega}{L_s'} \\ 0 & 0 & -\frac{p\Omega}{L_s'} & \frac{1}{L_s' \tau_r} \end{bmatrix} ;$$

with

$$D = \left(\frac{1}{L_s' \tau_r}\right)^2 + \frac{p^2\Omega^2}{L_s'^2} = \frac{1 + p^2\tau_r^2\Omega^2}{L_s'^2 \tau_r^2} ;$$

$$\Lambda^{-1}(\Omega) = \begin{bmatrix} 1 & 0 & 0 & 0 \\ 0 & 1 & 0 & 0 \\ 0 & 0 & \frac{1}{L_s' \tau_r D} & \frac{p\Omega}{L_s' D} \\ 0 & 0 & -\frac{p\Omega}{L_s' D} & \frac{1}{L_s' \tau_r D} \end{bmatrix} ;$$

$$S^{-1} C^T = \begin{bmatrix} 2\theta & 0 \\ 0 & 2\theta \\ \theta^2 & 0 \\ 0 & \theta^2 \end{bmatrix} ;$$

$$\Lambda^{-1}(\Omega) S_0^{-1} (C\hat{Z} - y) = \begin{bmatrix} 2\theta & 0 \\ 0 & 2\theta \\ \frac{\theta^2}{\frac{L_s' \tau_r}{D}} & \frac{-\theta^2 p\Omega}{\frac{L_s'}{D}} \\ \frac{\theta^2 p\Omega}{\frac{L_s'}{D}} & \frac{\theta^2}{\frac{L_s' \tau_r}{D}} \end{bmatrix} \begin{bmatrix} i_{s\alpha} - \hat{i}_{s\alpha} \\ i_{s\beta} - \hat{i}_{s\beta} \end{bmatrix}$$

The gains are:

1st gain: $2\theta\left(i_{s\alpha} - \hat{i}_{s\alpha}\right)$

2nd gain: $2\theta\left(i_{s\beta} - \hat{i}_{s\beta}\right)$

3rd gain: $\frac{\theta^2 L_s' \tau_r}{1 + p^2\tau_r^2\Omega^2}\left(i_{s\alpha} - \hat{i}_{s\varepsilon}\right) - \frac{\theta^2 p\Omega L_s' \tau_r^2}{1 + p^2\tau_r^2\Omega^2}\left(i_{s\beta} - \hat{i}_{s\beta}\right)$

4th gain: $\frac{\theta^2 p\Omega L_s' \tau_r^2}{1 + p^2\tau_r^2\Omega^2}\left(i_{s\alpha} - \hat{i}_{s\alpha}\right) + \frac{\theta^2 L_s' \tau_r}{1 + p^2\tau_r^2\Omega^2}\left(i_{s\beta} - \hat{i}_{s\beta}\right)$

5 SIMULATION RESULTS

5.1 Performance of the direct-field-oriented control adapted to the four-parameter system

Simulations are performed on a direct-vector drive of the induction motor. The reference speed path is 150 rad/s at the startup, with a load torque applied at time t_1 = 1.5s and t_2 = 5.5s.

The rotor speed and the load torque are shown in Fig.5. The setting parameters are:

Pmec = 1.1KW, U = 220V, Rr = 4.3047Ω,

Rs = 9.65 Ω, Ls = Lr = 0.4718H, M = 0.4475H,

Jm = 0.0293kg/m², In= 2.6A, fm = 0.0038Nm.sec/rad, P= 2, speed 1410 rpm;

Control loop:_Speed (Ω), Choice of poles: Ω_0=30, ξ=1.25, Parameters of PI controller: K_p=1.1619, K_i=12.0059.

The rotor speed tested for a variation of + 25% RR, rotor flux, speed control and flux estimation are shown in Figs 6-10. A satisfactory performance is obtained despite a temporal variation of the rotor speed and load torque. Despite the state speed error due to the change in the rotation direction of the rotor speed and load torque (Fig 8), the rotor speed and flux are correctly estimated.

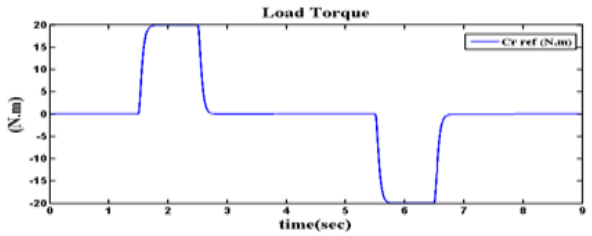

Figure 5. Reference speed and load torque.

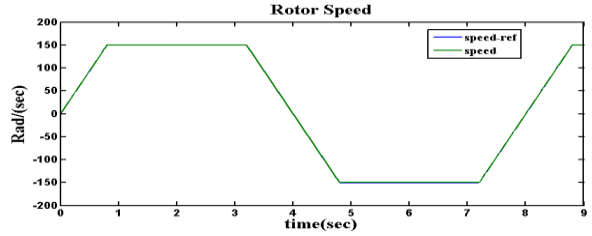

Figure 6. Rotor-speed control for a variation of +25% RR.

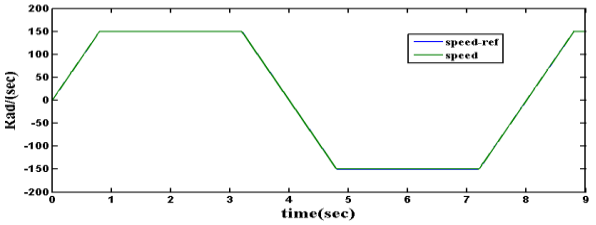

Figure 7. Rotor-speed for a variation of +25% RR.

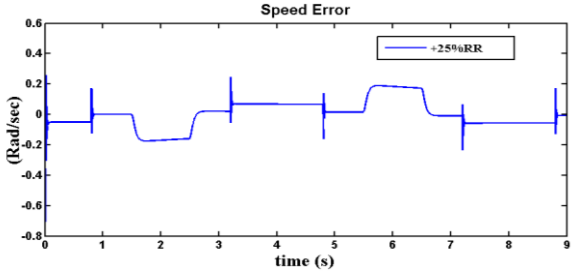

Figure 8. Error-speed control for a variation of +25% RR.

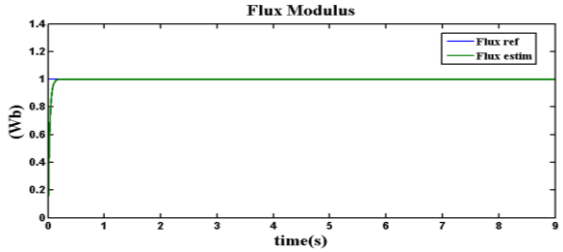

Figure 9. Flux modulus control at a variation of +25% RR.

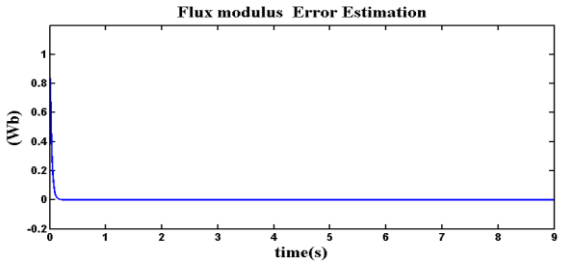

Figure 10. Rotor-flux estimation error for a variation of +25%RR.

5.2 Sliding-mode control in an open loop

The sliding mode controller is adapted to the four parameter-model of the induction motor. The flux is assumed to be measurable, and the controller is simulated for a change in the rotor resistance. The rotor speed error and rotor flux error are given in Figs 11-13. The variation does not affect the controller because the rotor speed error is less than 0.08 (rad/s).

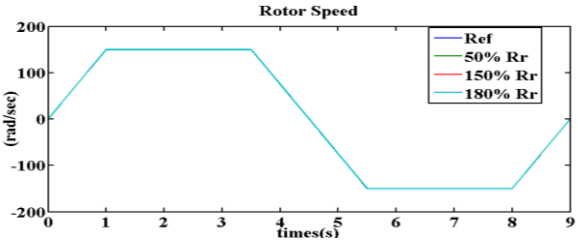

Figure 11. Rotor-speed at a +% RR variation.

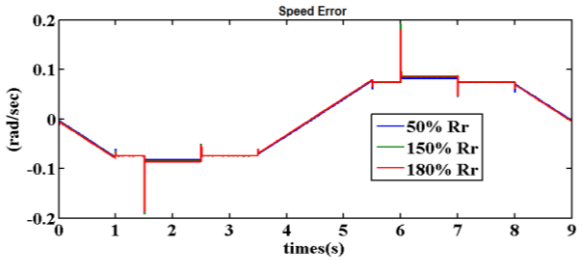

Figure 12. Rotor-speed error at a +% RR variation.

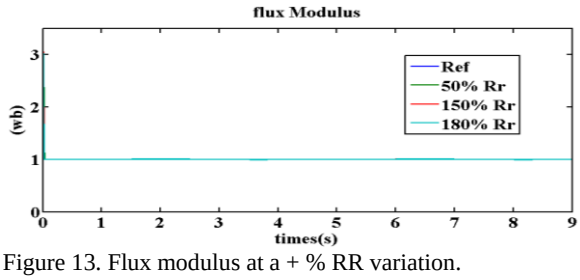

Figure 13. Flux modulus at a + % RR variation.

5.3 Performance of the high-gain observer control associated with the sliding-mode control

The nonlinear observer control is simultaneously simulated at a low and nominal speed. Fig. 14 shows the robustness and efficiency of the high-gain observer control adapted to a reduced motor model. The estimated flux follows its reference value perfectly despite the

variation in the rotor resistance over time. This is confirmed in Figs. 15 and 16 where the estimation error tends to zero after 0.02 s both at a low as well as at a nominal speed.

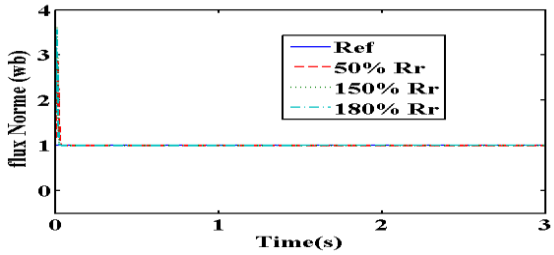

Figure 14. Flux modulus of a +% RR variation and low speed (230 tr/mn).

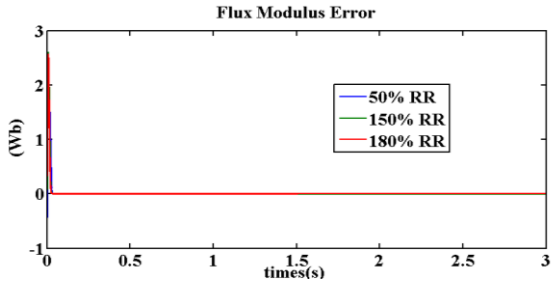

Figure 15. Flux error at a +% RR variation and low speed (230 tr/mn).

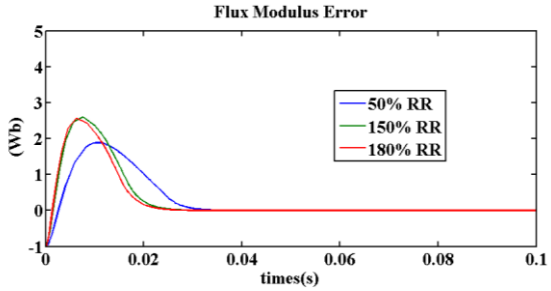

Figure 16. Flux error at a +% RR variation and nominal speed (150 rad/s).

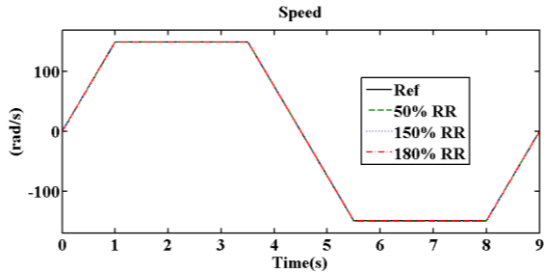

Figure 17. Nominal speed error at a +% RR variation.

6 VALIDATION

Our numerical simulations and results are validated compliantly with Benchaib et al. [10] and Hinkannen et. al. [16] using the same experimental conditions to ensure the similarity of the numerical results. The motor speed is evaluated as a function of time. A comparison between the results shows a very good satisfactory agreement.

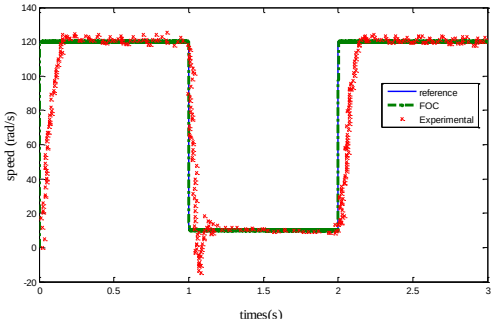

Figure 18. Comparaison between the obtained and the reference values [9].

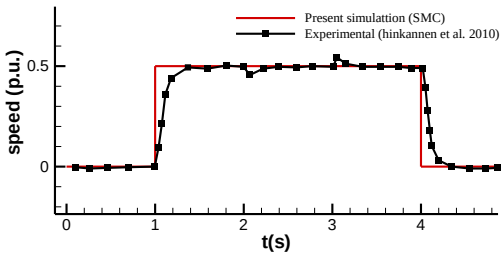

Figure 19. Comparaison between the obtained and the reference values [15].

7 CONCLUSION

Two robust control methods are used to setup a T-inverse model of the induction motor. The motor-model reduction technique is presented. The methods used to control the rotor speed and resistance variation give a good dynamic response in very low-speed domain. Applying a high gain nonlinear observer control proves their robustness in estimating the motor rotor flux. With the T-inverse there is no impact by the rotor inductance. Simulation results and validation under experimental conditions confirm the methods suitability for proposer. In future, the impact of the variation of the rotor resistance on the control will be experimentally verified and estimated for a possible adaptive control.

REFERENCES

[1] Mohamed Abid, Abdel Ghani Aissaoui, Boubekeur, Dehiba and Ahmed Tahour, ‘’Robustness Of Speed Adaptative Control For Asynchronous Machine”, Rev. Roum. Sci. Techn. – Électrotechn. et Énerg., 52, *2*, p. 241–251, Bucarest, 2007.

[2] H. Kubota and K. Matsuse, “Speed sensorless field-oriented control of induction motor with rotor resistance adaptatio”, *IEEE Trans. on Industry Applications*, v.30, no.5, 1994, pp. 1219-1224

[3] Abdellah. Mansouri, Mohammed Chenafa, Abderrahman. Bouhenna, and Eric. Etien, “Powerful nonlinear observer associated with field-oriented control of an induction motor”, Int. J.A.M.C.S., Vol. 14, No. 2, pp. 209–220, 200.

[4] Marko. Hinkkanen, “Flux Estimators for Speed Sensorless Induction Motor Drives”, Espoo 2004Elektrotehniški vestnik online, http://ev.fe.uni-lj.si (1.1.2014).

[5] Imene Kebbati, Yamna Hammou, and Abdalla Mansouri, “Sliding mode control with a robust observer of an induction motor”, *Przeglad Elektr.*, Vol. 1b, pp. 193–197, 2012.

[6] Yama. Hammou, Imene Kebbati and Abdallah. Mansouri, “New Algorithms of Control and Observation of the Induction Motor Based on the Sliding-Mode Theory”, Electric Power Components and Systems, 43:5, 520-532, DOI: 10.1080/15325008.2014.99207.

[7] Hinkkanen, M. & Leppanen, V.-M. and Luomi, J., “Flux Observer Enhanced With Low-Frequency Signal Injection Allowing Sensorless Zero-Frequency Operation of Induction Motors”,IEEE Transactions on Industry Applications. Volume 41, Issue 1. 52-59. ISSN 0093-9994 (printed). DOI: 10.1109/tia.2004.840958.

[8] Hinkkanen, M. & Luomi, J. “Braking Scheme for Vector-Controlled Induction Motor Drives ”,IEEE Transactions on Industry Applications. Volume 42, Issue 5. 1257-1263. ISSN 0093-9994 (printed). DOI: 10.1109/tia.2006.880852.

[9] Slotting, J.J.E., and Sastry, S. S., “Tracking Control of Nonlinear Systems using Sliding Surfaces with Application to Robot Manipulators”, Int. J. Control, 38(2), 1983.

[10] Abdlekrim Benchaib, Ahmed Rachid, E. Audrezet and M. Tadjine, “Experimental Evaluation of Sliding Mode Induction Motor Contro”, IEEE explore print ISBW 978-3-952 4269-0-6, (2015).

[11] Hassan. Hammouri and Mondher. Farza, “Nonlinear Observers For locally Uniformly Observable Systems, ESAIM: Control, Optimisation and Calculus of Variations”, March 2003, Vol. 9, 353-370.

[12] Fenglong. Liu, Mondher. Farza and Mohammed. M’saad, “ bservateur à grand gain pour des systèmes non linéaires avec couplage non complètement triangulaire”, schedae 2007.

[13] Abdellah. Mansouri, Mohammed Chenafa, Abderrahman. Bouhenna, and Eric. Etien, “Powerful Nonlinear Observer Associated with control of Induction Motor”, Int. J. Appl. Math. Compute. Sci., 2004, vol. 14, No.2, 209-220.

[14] Qu. Zengcai; Marko. Hinkkanen and Harnfors Lennart, “Gain scheduling of a full-order observer for sensorless induction motor drives”, IEEE Transactions on Industry Applications, 50(6), 3834-3845. DOI: 10.1109/TIA.2014.2323482, 2014.

[15] R.Saravana Kumar, K.Vinoth Kumar and Dr. K.K.Ray, “Sliding Mode Control of Induction Motor using Simulation Approach”, IJCSNS International Journal of Computer Science and Network Security, VOL.9 No.10, October 2009.

[16] Hinkkanen, L. Harnefors and J.Luomi, “Reduced-Order Flux Observers With Stator-Resistance Adaptation for Speed-Sensorless Induction Motor Drives”. IEEE Transactions on Power Electronics. Volume 25, Issue 5. 1173-1183. ISSN 0885-8993 (printed). DOI: 10.1109/tpel.2009.2039650, 2010.

[17] Lennart Harnefors, »Design and Analysis of General Rotor-Flux-Oriented Vector Control Systems“, IEEE Transactions on Idustriel electronique, Vol. 48, No. 2, April 2001.

[18] R. Yazdanpanah, J. Soltani and G.R. Arab Markadeh, “Nonlinear torque and stator flux controller for induction motor drive based on adaptive input–output feedback linearization and sliding mode control”, Elsevier 2007.

[19] Vasyl Malyar, Orest Hamola, Volodymyr Madai, Ivanna VasylchyshynMathematical “Models to Study Series Compensation of the Induction-Motor Reactive Power ”, ELEKTROTEHNIŠKI VESTNIK 88(5): 285-289, 2021 ORIGINAL SCIENTIFIC PAPER.

[20] Ricardo. Marino, Patrizio.Tomei and Cristiano. Maria. Vercelli, A New Flux Observer for Induction Motors with On-Line Identification of Load Torque and Resistances, Preprints of the 18th IFAC World Congress Milano (Italy) August 28 - September 2, (2011).

[21] Mohan. Krishna S, Febin and Daya. J. L, Sanjeevikumar. Padmanaban and Lucian. Mihet. Popa, Real-Time Analysis of a Modified State Observer for Sensorless Induction Motor Drive Used in Electric Vehicle Applications, Energies (2017).

[22] G. C. Verghese and S. R. Sanders, “Observers for flux estimation in induction machines”, IEEE Trans. Ind. Electron., vol. 35, no. 1, pp. 85–94, Feb. (1988).

[23] D. H. Popovic, I. A. Hiskens and D. J. Hill, “Stability Analysis of Induction Motor Network”, Electrical Power &Energy System, Vol, 20, No 7, pp, 475-487. (1998).

[24] G.R. Selemon, “Modeling of induction machines for electric drives”, IEEE Trans. on Industry Applications, v. 25, no. 6, 1989 pp. 1126-1131.

[25] V. Utkin, J. Guldner anJ. Shi, “Sliding mode control in electromechanical systems”, Taylor & Francis, (1999).

[26] Fenglong Liu, Mondher Farza, Mohammed M’saad “Observateur à grand gain pour des systèmes non linéaires avec couplage non complètement triangulaire”.

[27] Mondher. Farza, I. Bouraoui, Tomas. M’enard, Ridha. Ben Abdennour and Mohammed. M’Saad, “Sampled output observer design for a class of nonlinear systems”, Control Conference (ECC), European, Strasbourg, France. pp.312 - 317, (2014).

Ymene Kebbati received her postgraduate degree in 2006 and her PH.D. degree in 2012 from the Faculty of Electrical Engineering, University of Sciences and Technologies of Oran (USTO)-Algeria-. She works in electro-mechanical control systems. Since 2014, she is currently working as a senior lecturer at the University of Sciences and Technologies of Oran, her research interest is the efficiency control of electrical machines and drives.

Yamna Hammou received her PH.D. degree in 2015 from the National Polytechnic School of Oran (ENPO) -Algeria-. She works in electro-mechanical control systems. Since 2015, she is currently working as a senior lecturer at the Faculty of Mechanical Engineering, University of Sciences and Technologies of Oran (USTO), her research interest is the efficiency control of electromechanical machines.